

# An A-Train Convective Object Database for Studying Atmospheric Convective Processes

Juliet Pilewskie<sup>1</sup> and Tristan L'Ecuyer<sup>1</sup>

<sup>1</sup>University of Wisconsin-Madison | contact: pilewskie@wisc.edu



## Introduction

- Atmospheric deep convection contributes to the Earth's climate through precipitation and cloud properties
  - Latent heat is released when convective systems precipitate to form an approximate balance with radiative cooling on a global scale
  - Convective clouds have competing SW and LW radiative effects, and whether they warm or cool the Earth constitutes the sign of the **high cloud feedback** (Stephens, 2005)
- Models contain large uncertainties in high cloud feedbacks due to the challenge of acquiring global-scale observations that capture convective behavior at fine spatial and temporal scales
- The A-Train, despite only twice-daily sampling, is able to capture cloud properties, precipitation, and radiative effects of convection on a nearly global scale

## Guiding Questions

- How representative is A-Train-observed convection compared to previous spaceborne radar-based analyses (Zipser et al., 2006)?
- What added insight on convection can the A-Train provide?

## Methods for Characterizing Convective Systems

A "cloud object" approach is used to identify all convective systems between August 2006 – December 2010 in the following manner:

- Convective cores are identified based on the height of the attenuating reflectivity (Z) profile from CloudSat's 94 GHz CPR
- Contiguous "cloudy" pixels with dCTH < 1.5 km surrounding the cores are stored as "convective objects" (COs)
- Variables defining vertical intensity, horizontal extent, convective core properties, precipitation, and radiative response are calculated over the CO

- Relative Center of Gravity (CoG)** defines the vertical intensity and is the height at which the mean Z-weighted mass of the core is located subtracted by the height of the freezing level

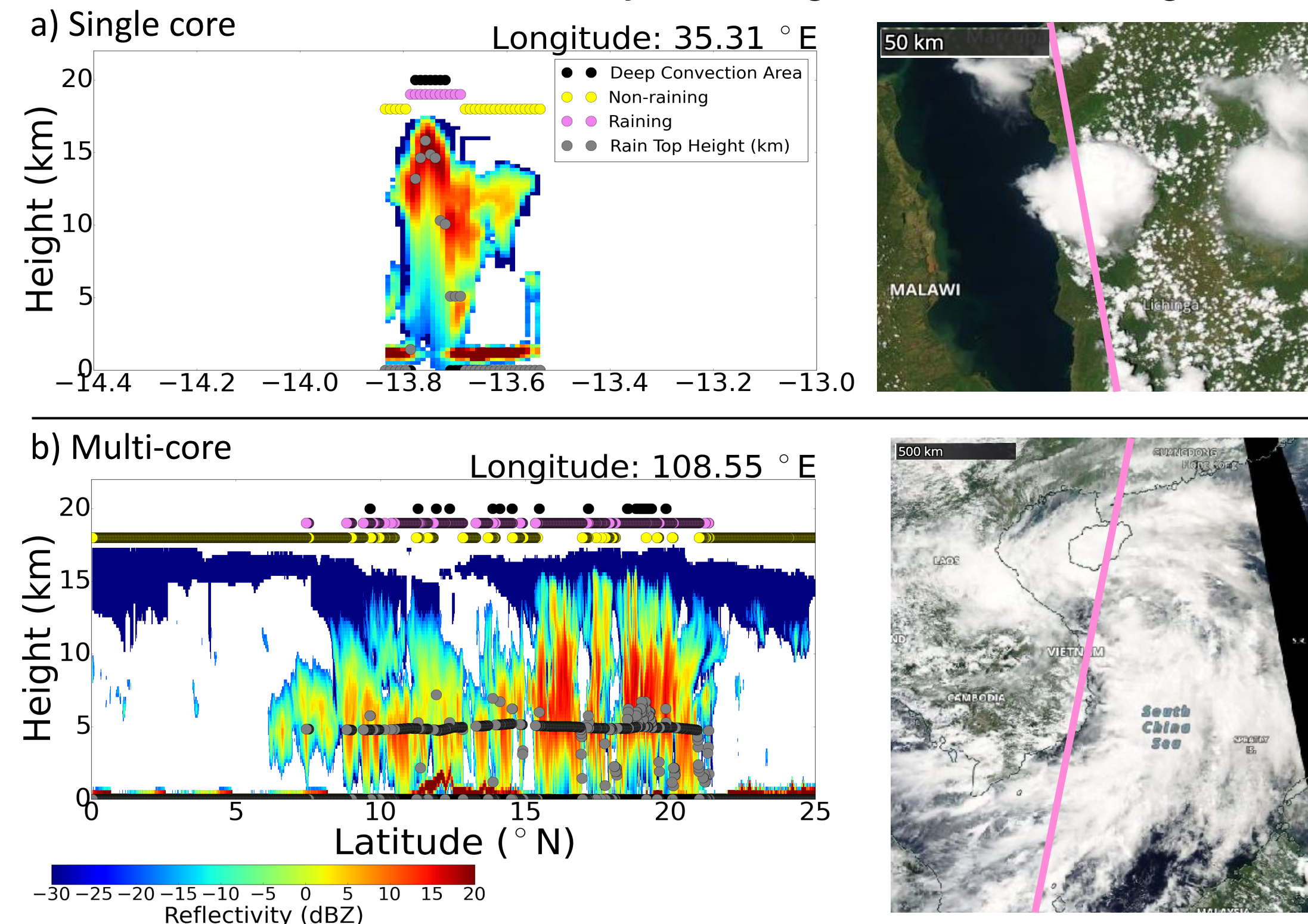


**Fig. 1:** Left: Reflectivity profiles of *single core* (top) and *multi-core* (bottom) COs with colored markers indicating deep convection region, non-raining and raining anvil regions, and rain top heights. Right: MODIS-corrected reflectances of each event with CloudSat flyover overlaid in pink.

## Where and when does convection occur most frequently?

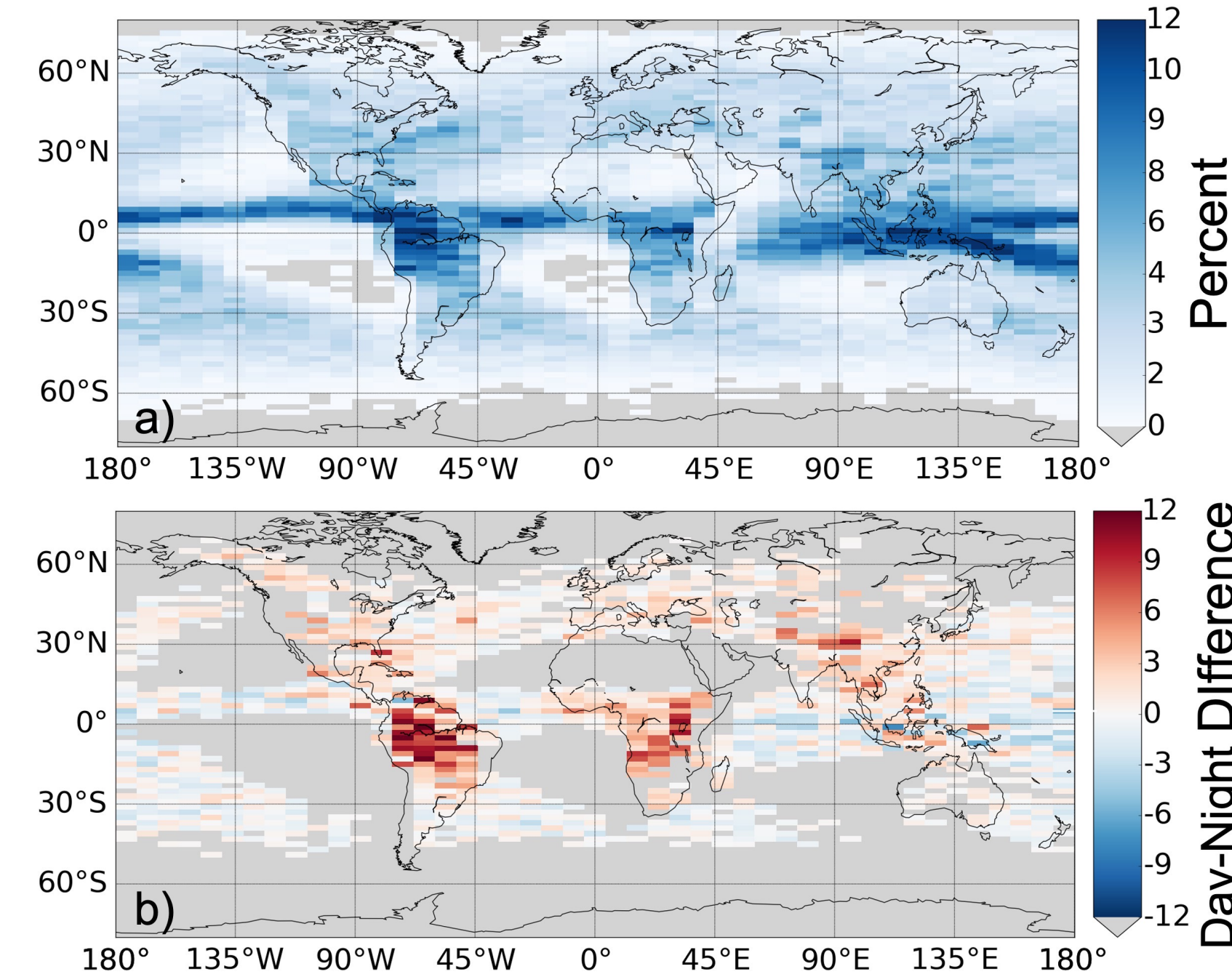
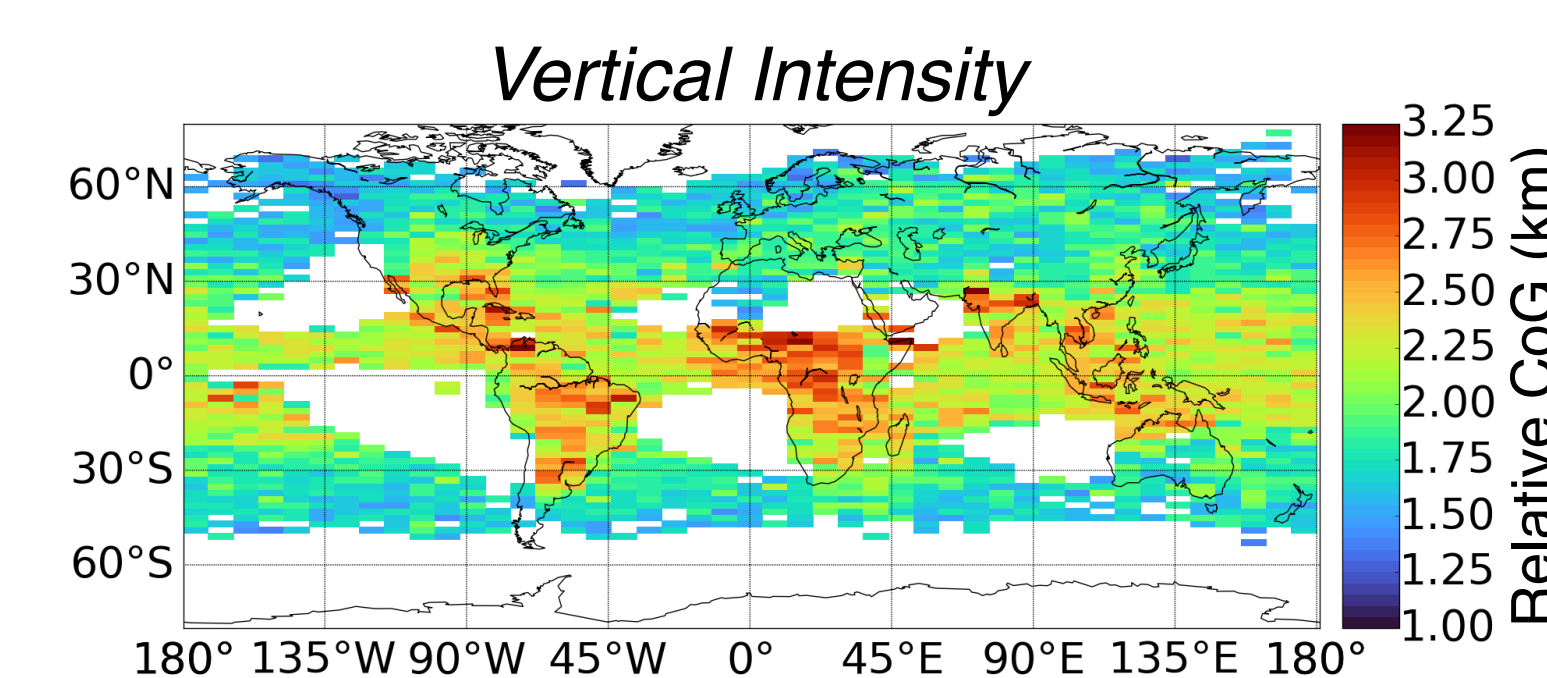


**Fig. 2:** (Top) Frequency of convective objects and (bottom) difference in convective object frequencies between 1:30 pm and 1:30 am within 8°x2° grid boxes.

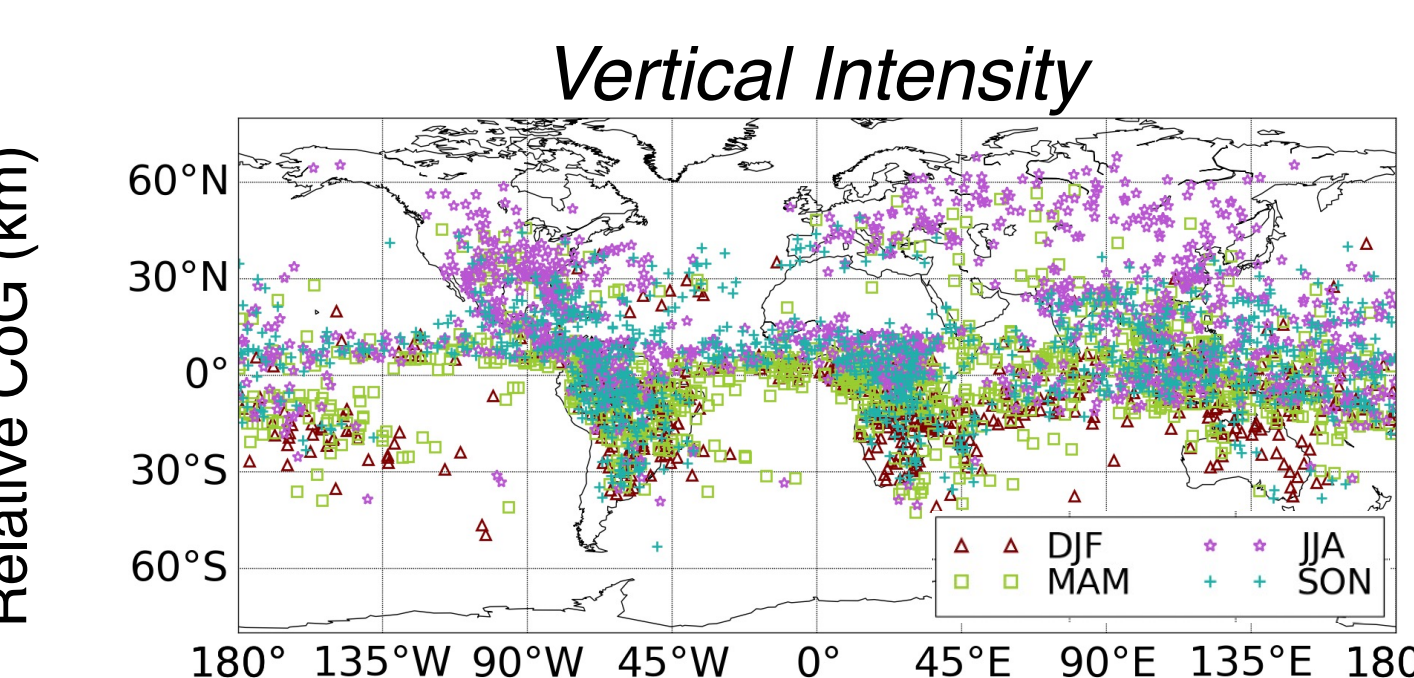
- 95,520 COs are observed
- COs are most prevalent in the tropics** over the Amazon, Congo Basin, Maritime Continent, and along the ITCZ
- Early afternoon convection is more prevalent over land in the tropics, while early morning convection is more common over tropical ocean
- The A-Train observes that convection peaks in the early afternoon east of the Rocky Mountains and over the Tibetan Plateau, as shown in previous studies (Xu & Zipser, 2011)

## What is the global variability in cloud features and precipitation?

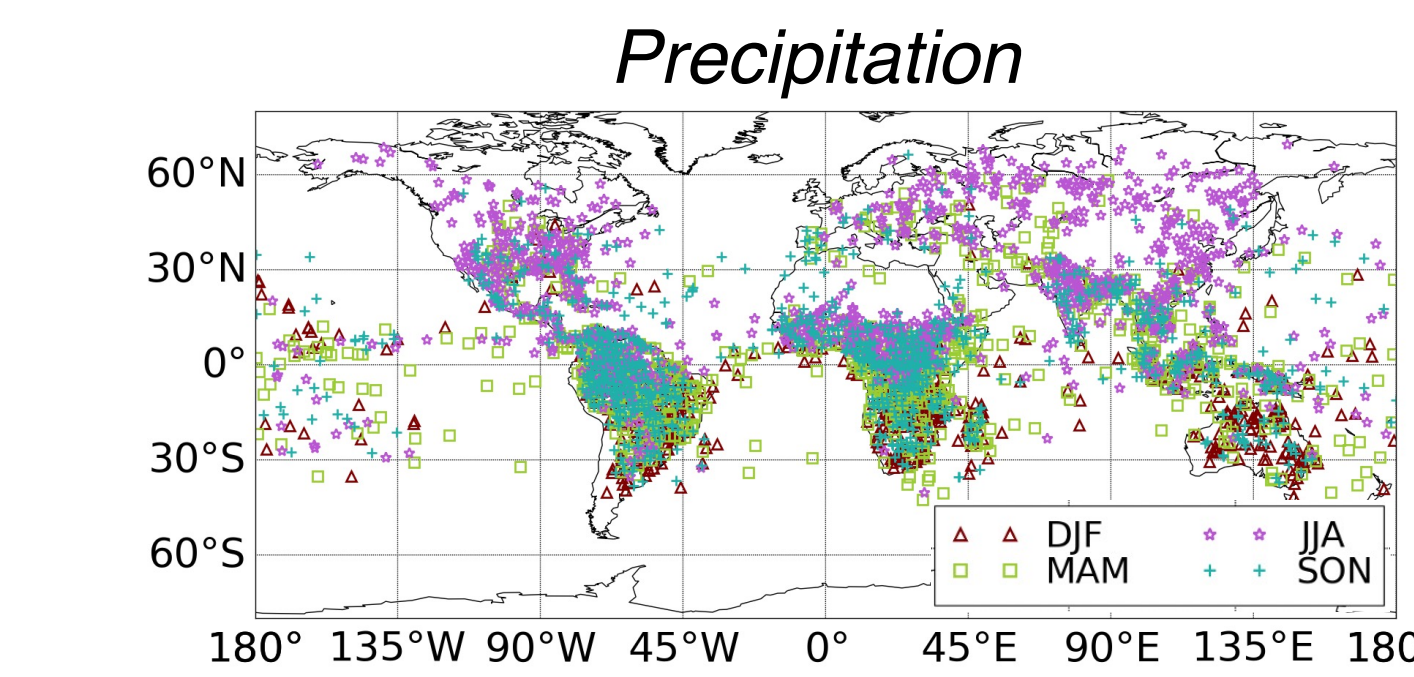
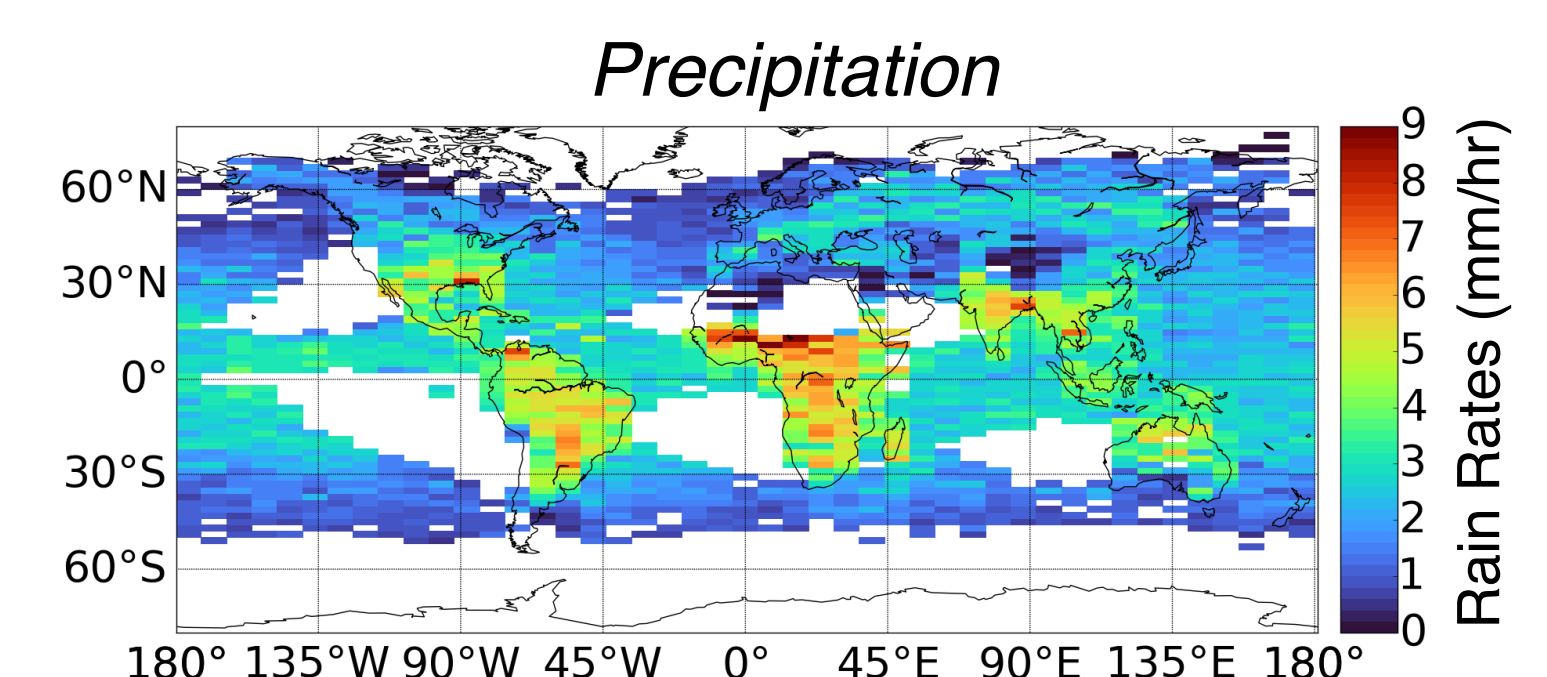
### 1. Mean distribution of COs



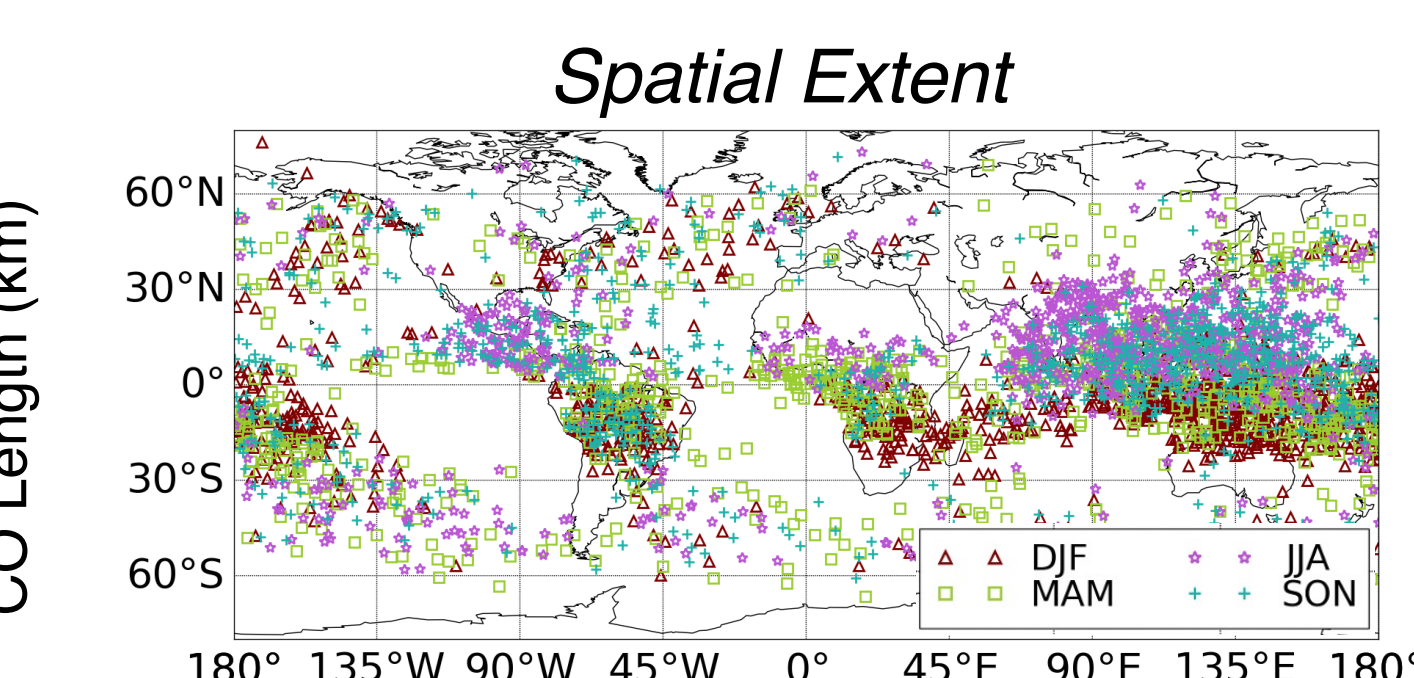
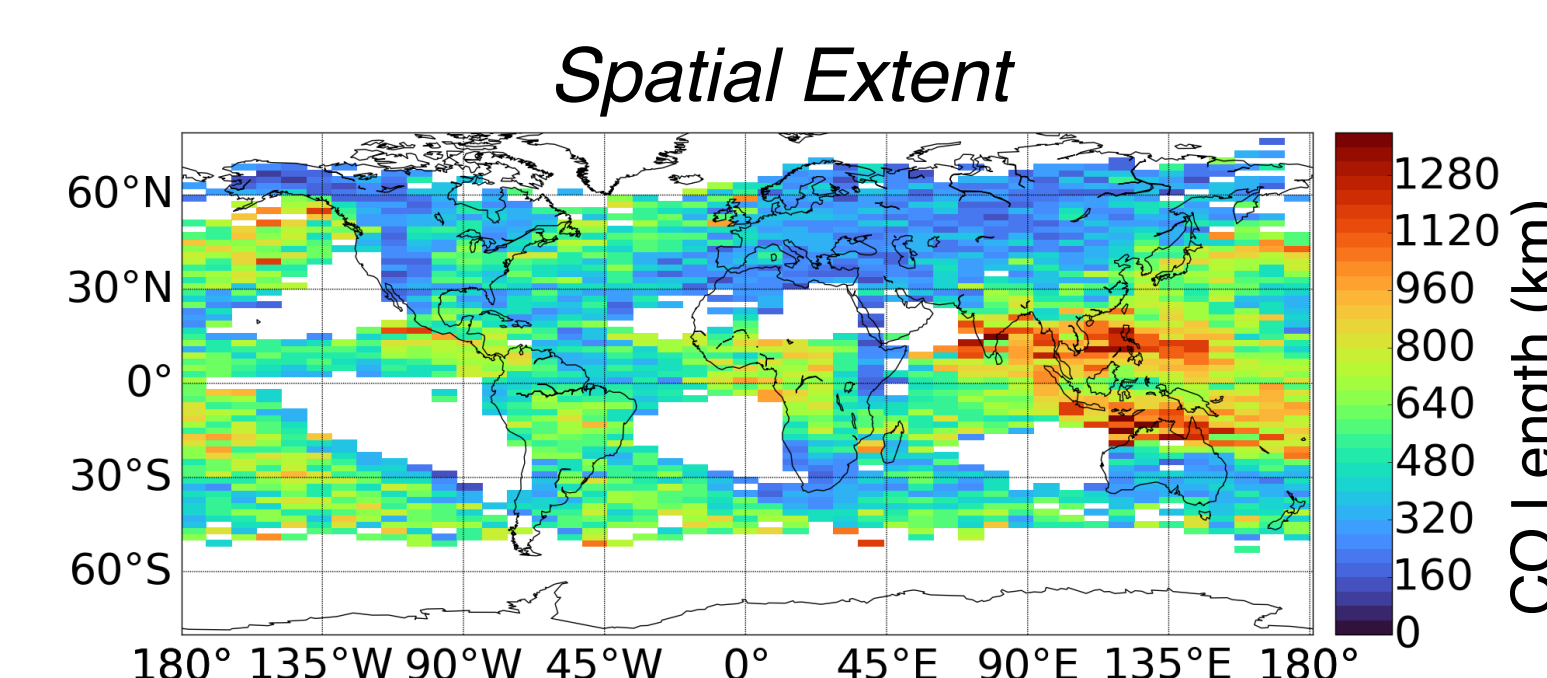
### 2. 5% most extreme COs by season



While the most intense convection occurs predominantly over tropical land, there is a **large prevalence of the most intense convection occurring over mid- and high latitude land during boreal summer.**



The spread in the heaviest rainfall rates follows closely to that of vertical intensity, but the **heaviest rainfall rates are confined to land only.**



**COs with the longest extent** occur over Southeast Asia, the Maritime Continent, and the Indian and West Pacific Oceans, and their locations follow the seasonal shift in the ITCZ.

**Fig. 3:** (Left) Means within 8°x2° grid boxes of, and (right) seasonal differences for the top 5%, (top row) relative core CoG, (middle row) AMSR-E rain rates, and (bottom row) CO length along CloudSat overpass.

## How do clouds and radiation correspond to core prevalence?

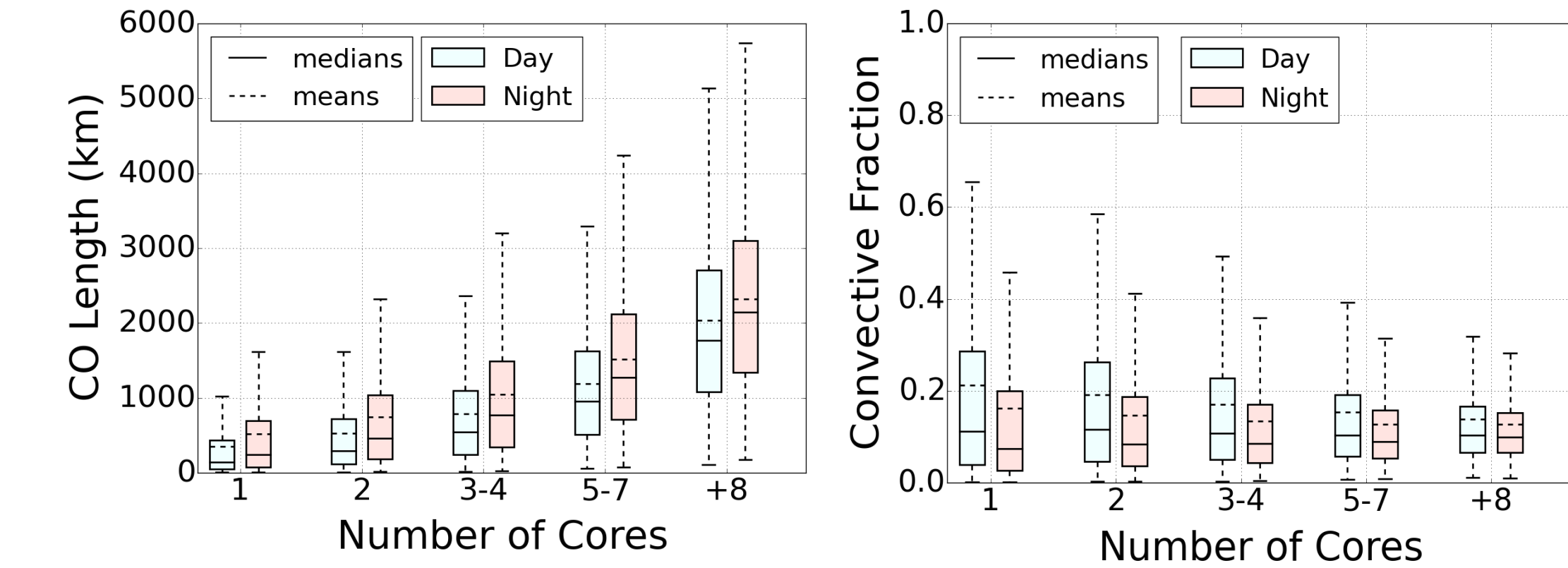
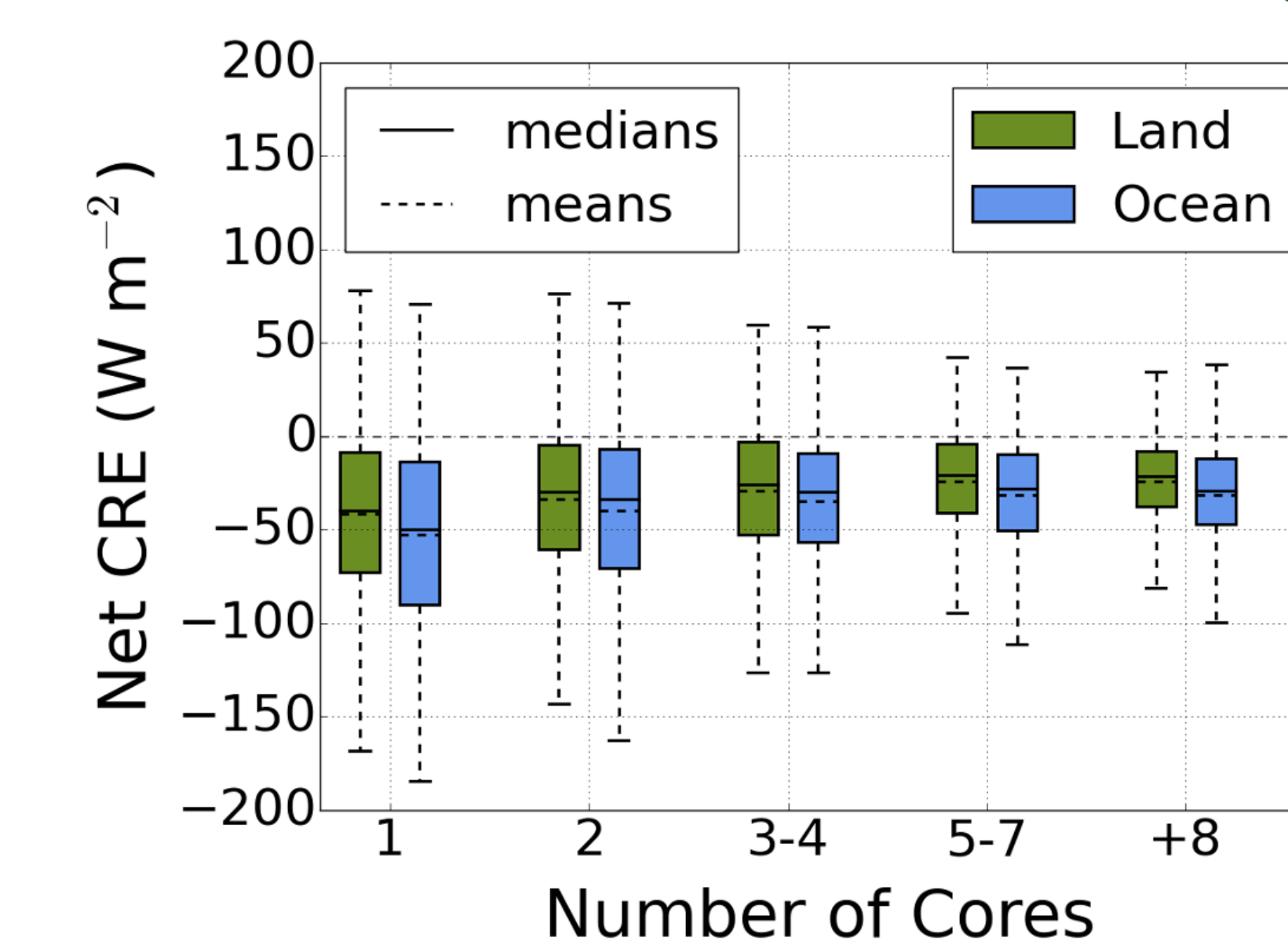


**Fig. 4:** Box-whisker plots showing (left) CO length, and (right) convective fraction for day and night A-Train overpasses sorted by the number of deep convective cores in each system over the whole globe.

Non-convective anvil cloud extent increases as the number of embedded cores increase. **What are the resulting radiative effects of these COs?**



COs have a cooling impact with **single-core systems having the largest cooling impact.** Cooling does not significantly weaken as the number of embedded cores increase suggesting that processes beyond internal convective dynamics influence anvil radiative effects.

**Fig. 5:** Box-whisker plot showing daytime (1:30 pm) convective object net CRE over land and ocean between 30°S and 30°N and sorted by the number of deep convective cores in each system.

## Future Work

- Do the differences in anvil thickness help explain the large spread in CRE?
- How do the links between convective characteristics, precipitation, and radiative effects vary as a function of the environment?
- How do the energetics of convection differ at the varying life-cycle stages?

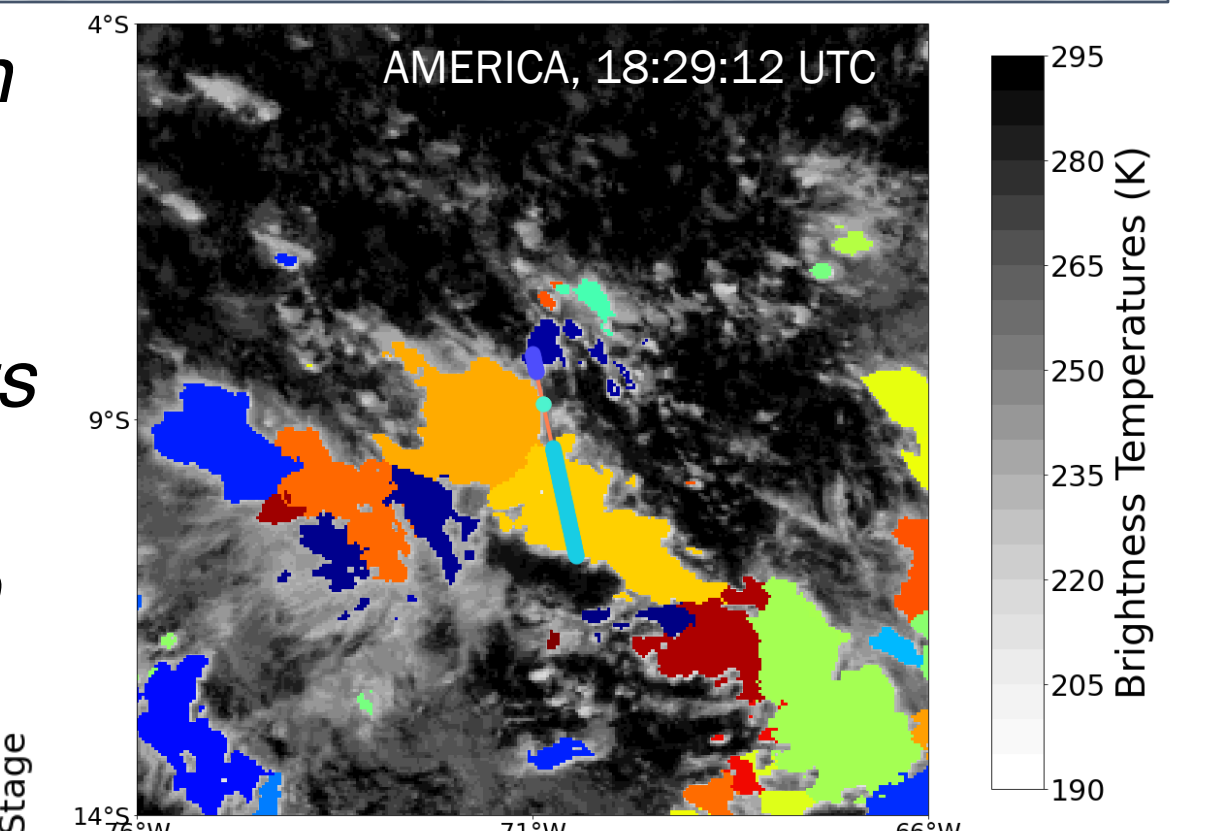
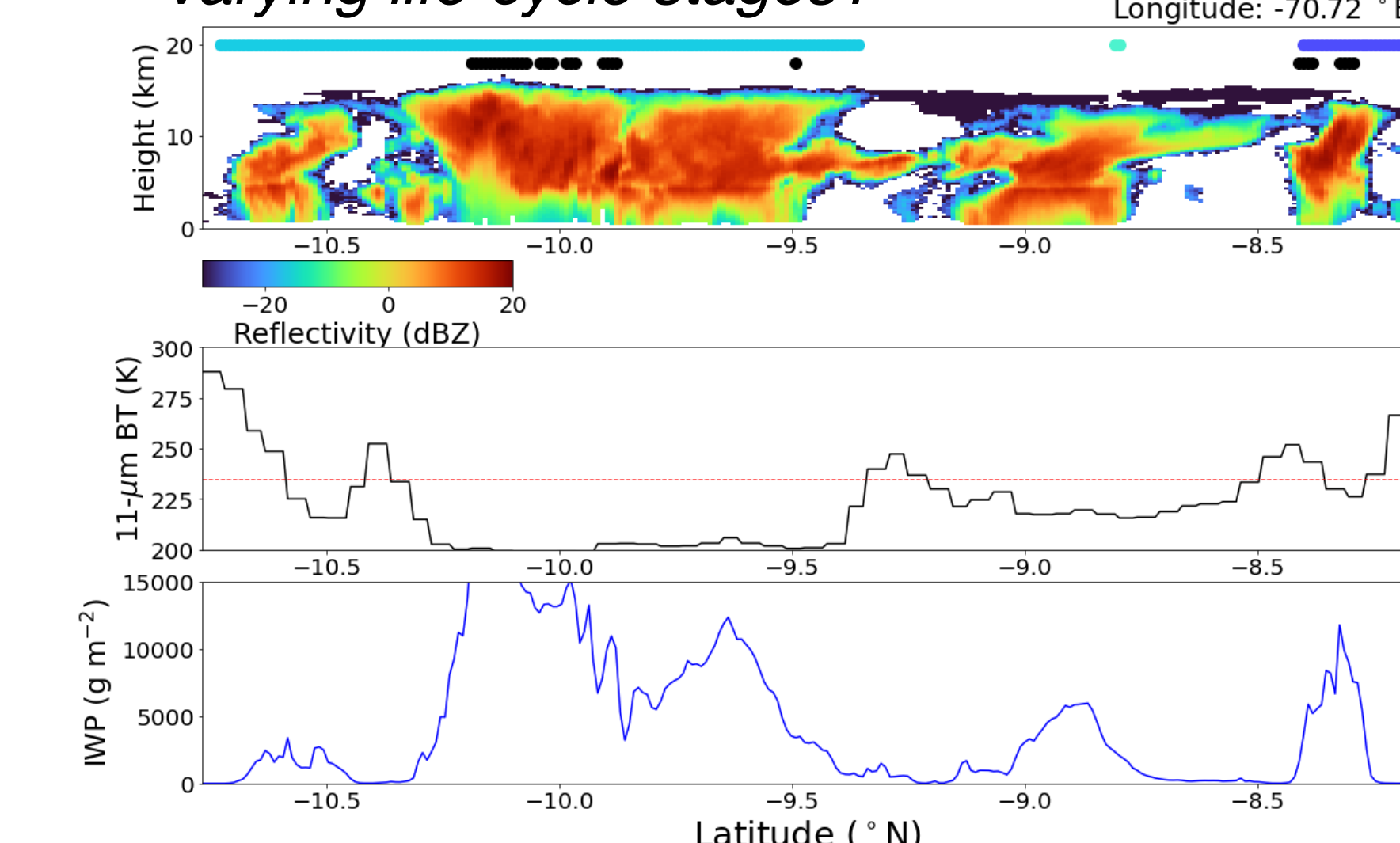


**Fig. 6:** Top: 4-km GPM-MERGIR brightness temperatures (BTs) with distinct MCSs from Tracking Of Organized Convection Algorithm (TOOCAN; Fiolleau and Roca, 2013) overlaid in color. Left: CO quicklook of (top) reflectivities with markers indicating TOOCAN-MCS life-cycles, (middle) MODIS BTs, and (bottom) column-integrated ice water path.

## References

- Fiolleau, T. and R. Roca (2013). *IEEE TGRS*. 10.1109/TGRS.2012.2227762.
- Pilewskie, J. and T. L'Ecuyer (2022). *JGR Atmospheres*. e2022JD036438.
- Stephens, G. L. (2005). *Journal of Climate*. 10.1175/JCLI3243.1.
- Xu, W., & Zipser, E. J. (2011). *Journal of Climate*. 10.1175/2010JCLI3719.1.
- Zipser, E. J. et al., (2006). *BAMS*. 10.1175/BAMS-87-8-1057.

## Acknowledgements

This research has been supported by the NASA Science Mission Directorate through the FINESST program (Award no. 80NSSC20K1651) and the NASA Jet Propulsion Laboratory (CloudSat Grant no. G-39690-1).